

MICROSTRUCTURAL ELEMENTS OF COMPONENTS DERIVED FROM 3D PRINTING

M.J. Cima, A. Lauder, S. Khanuja, and E. Sachs

Departments of Materials Science and Engineering and Mechanical Engineering,
Massachusetts Institute of Technology, Cambridge, MA 02139

ABSTRACT

Three Dimensional Printing is a rapid prototyping technique to manufacture functional components directly from computer models. The process involves spreading the powder in thin layers and then selective binding of the powder using a technology similar to ink-jet printing. Layers are added sequentially until a part is completed. The simplest microstructural feature of a 3DP part results from the interaction of a binder droplet with the powder bed; termed as "primitive." These primitives have denser powder packing than is found in the loose powder bed. Formation of the primitives is found to be dependent on the physical and chemical characteristics of the powder and binder. The present study discusses the effect of size, morphology and packing density of different alumina powder on the microstructural features and densification of the primitives.

INTRODUCTION

Solid Freeform Fabrication (SFF) techniques are largely viewed as methods for replicating macroscopic structures derived from computer descriptions of solid models. One can envision, however, components where both the *macrostructure* and *microstructure* are designed by computer. Never before have materials engineers had complete freedom to design microstructures. Microstructure is usually developed within the confines of the manufacturing process. Thus, designers must compromise component performance with manufacturability. SFF processes build components on a point-by-point basis and may make it possible to vary the composition and structure of a component from position to position with complete freedom. Potential applications of such a technology are numerous, such as components with anisotropic thermal, electrical, or mechanical properties or microengineered porosity. This paper is one of a series in which the basic microstructural features of 3D Printed components are discussed [1,2]. Knowledge of the physical processes which control the microstructure of 3D Printed parts will aid in its use as a tool for the production of microengineered materials.

3D Printing is among those rapid prototyping technologies that deposit matter during the building process. Thus, it can selectively control composition within the build plane by varying the composition of printed material. Significant amounts of matter can be deposited in selective regions of a component on a 100 μm scale by printing solid dispersions or solid precursors through the ink-jet. Multiple jets of different composition

or concentration could be employed to prepare components with composition and density variation on a fine scale. A recent study has shown that several factors contribute to the formation of 3DP microstructure [1]. Experiments were carried out to trace the development of the microstructure from its smallest units to a complete part by examining single-droplet primitives, lines formed by printing binder in a continuous bead across the powder bed, and walls prepared by printing lines close enough together that they binder to form macroscopic structures. Single-droplet primitives are the structures created when a single binder droplet impacts the powder bed. The ballistic impact of the binder droplets causes cratering and ejection of powder over a large distance [2]. Capillary action draws liquid into the powder in cases where the liquid wets the powder surface. If, however, the capillary stress exceeds the cohesive strength of the powder bed then significant particle rearrangement will occur as the particles are drawn into the liquid [1]. Thus, the microstructure is largely the result of the relative influence of capillary and cohesive forces.

This study reveals the relationship between the structure of single droplet primitives and the nature of the powder used in the piston. The primitive size, morphology, and packing density were characterized for several powders that could be useful for making investment casting molds and cores by 3D Printing [3,4].

EXPERIMENTAL PROCEDURE

The powders used in this study are described in Table 1. Colloidal silica (Nyacol 830, Nyacol Products Inc., Ashland, Massachusetts) was used as the binder for all experiments.

Primitives were prepared by using a 3D printing machine which is described elsewhere [5]. The printhead used for this study was the continuous-jet type. Thus, droplets are produced continuously at 50 to 60 kHz. These droplets are selectively charged by applying a voltage between the binder and the charging plates that are placed near the jet orifice. Charged droplets are deflected when passed between high voltage deflection plates. Uncharged droplets proceed unimpeded until they impact the powder bed. A special circuit was designed to drive the charging cell. This circuit allowed only one droplet out of every 32 to remain uncharged and strike the powder bed. The printhead was driven over the powder bed at a velocity of 2.5 m/s in a raster fashion with trajectories separated by 780 μm . Thus, neighboring droplets along a line were separated by almost 0.8 mm and were too far apart to stitch together. Powder was spread over the piston in layers, 380 μm thick. Complete coverage of 90 x 90 mm powder bed produced more than 10,000 primitives per layer. The powder was carefully scooped out of the piston after printing and fired at 900° C for 2 hours. The fired powder was then passed through several sieves of different mesh sizes to separate the primitives from the unbound powder.

Three sets of experiments were used to characterize primitives. Skeletal density measurements were conducted by a helium pycnometer (Quantachrome, Syosset, NewYork). The sample size varied between 2 and 4 g. Pycnometer measurements were

taken using pressures of approximately 140 kPa. Repeated measurements were taken until three values for sample volume agreed within 1%.

Microscopic analysis of the primitives was performed by scanning electron microscopy (SEM). These samples were prepared by affixing a few milligrams of primitives on aluminum stubs using adhesive press tabs followed by gold coating in a sputter coater.

Mercury porosimetry was used to determine the bulk density and pore-size distribution of the primitives. Measurements were made using an automated porosimeter (Micromeritics, Norcross, Georgia). The penetrometer was loaded with primitives and evacuated to a pressure of 50 $\mu\text{m-Hg}$. The chamber was then filled with mercury at a pressure of 21.6 kPa. High pressure infiltration of mercury was then used to determine the total infiltration volume. Accurate calculation of the average primitive density required that a correction be applied to the infiltration volume since, in some cases, the low pressure infiltration was not sufficient to completely infiltrate the inter-primitive pores. The details of the data correction are described elsewhere [6]. Briefly, the infiltration volume of the intraprimitive pore space was taken as the difference between the total infiltration volume and the infiltration volume at the pressure required to begin infiltration of the loose alumina powder from which the primitives were made. The operative assumption is that the primitives contain no pores that are larger than the largest pores found in the loose powder

Powder	Average size (microns)	Shape
Norton 325 mesh alumina*	45	Faceted gravel-like
Norton 30 micron alumina*	30	Hexagonal plates
Spray dried alumina	15	Porous spheres
ICD alumina #	10	Solid spheres

* Norton Company, Waltham, Massachusetts.

ICD Group, Lyndhurst, New Jersey

RESULTS AND DISCUSSION

Single drop primitives, regardless of the powder used, were found to be roughly spherical in shape. Primitives prepared from spherical powders are noticeably larger than those from irregular shaped or plate-like powders. Those primitives prepared from the spherical ICD alumina had diameters between 200 and 300 μm . The spray-dried and angular shaped powders, however, gave primitive diameters between 100 and 200 μm . Figures 1 and 2 are primitives made from 325 mesh alumina and ICD alumina, respectively. High magnification observation of primitives, Figure 3 and 4, reveal how the particles are bound by the silica. Irregular powders generally bond across large flat faces with silica wetting across the entire bond. Spherical powder, however, is bonded by small amounts of silica at the necks between the particle spheres.

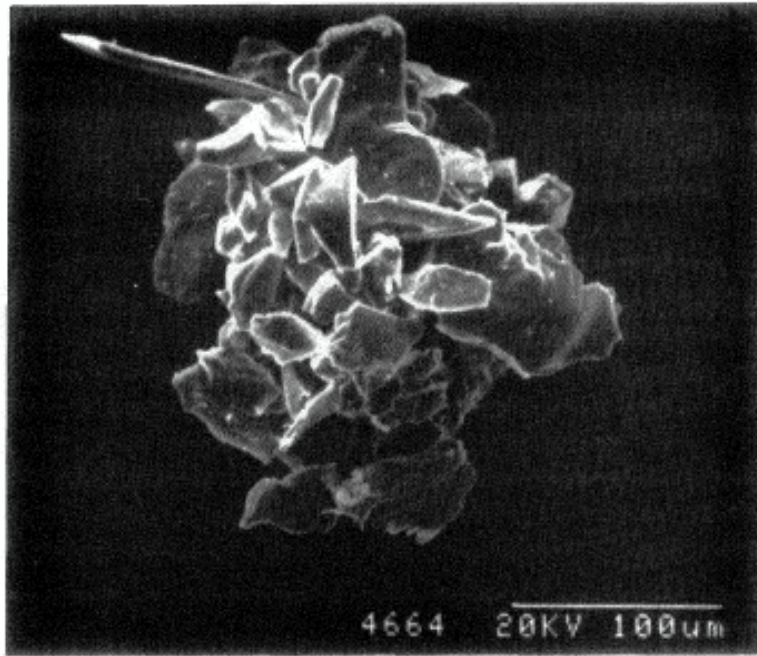


Figure 1. Micrograph of a single drop primitive made from 325 mesh alumina.

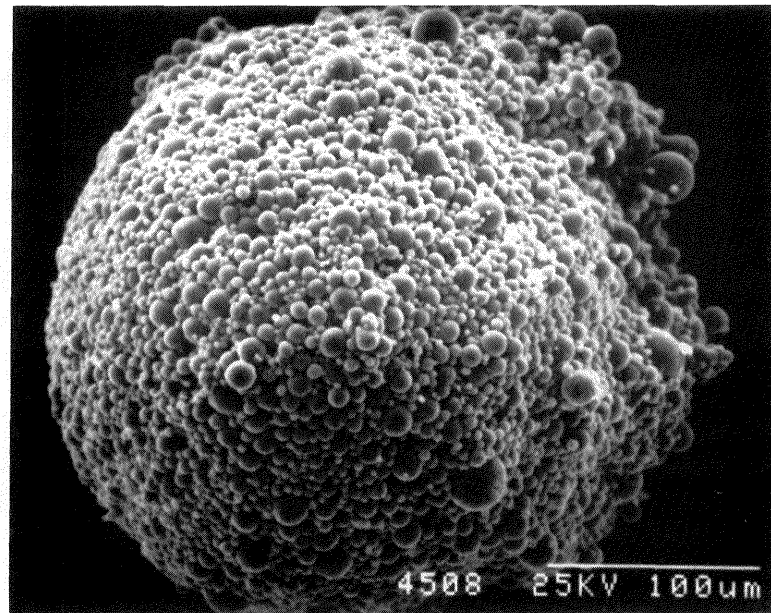


Figure 2. Micrograph of a single drop primitive made from ICD alumina.

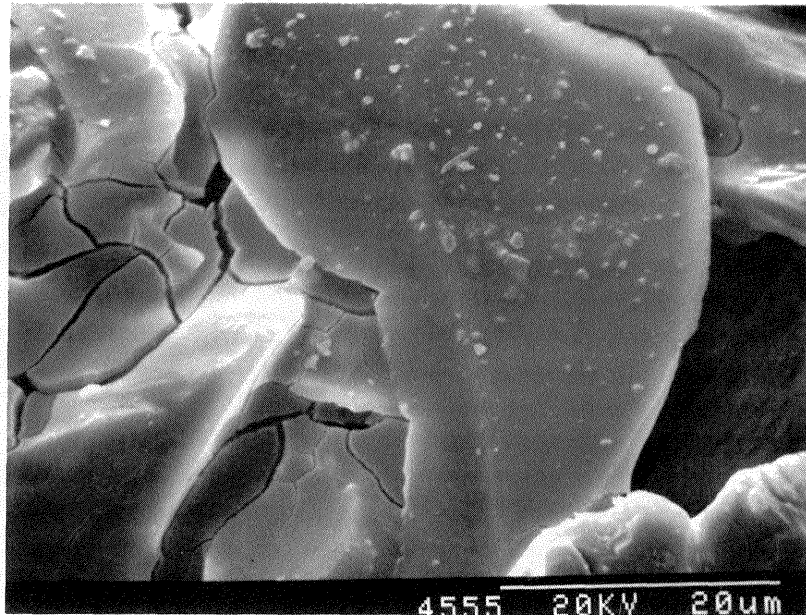


Figure 3. High magnification of the surface of a primitive made out of faceted 325 mesh alumina.

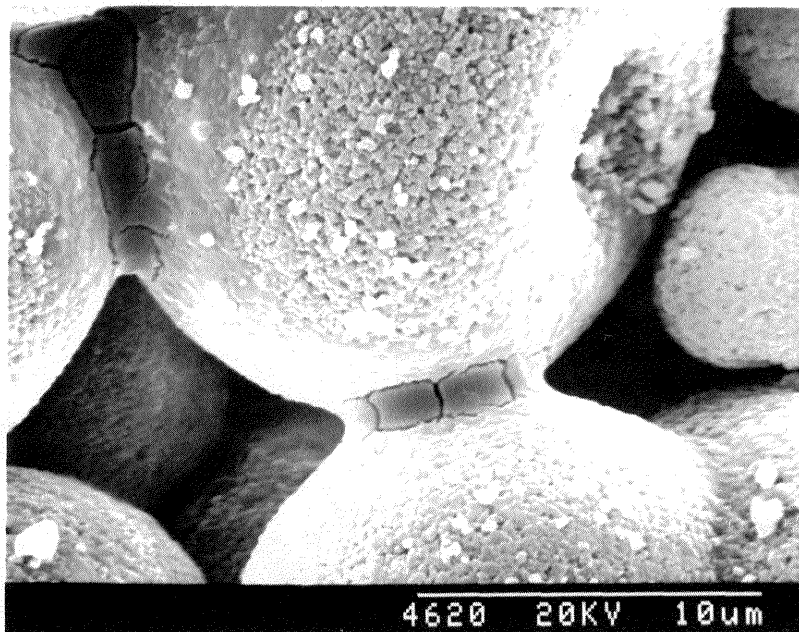


Figure 4. High magnification of the surface of a primitive made from spherical spray dried powder

Skeletal density data for individual primitives can be used to determine the relative amounts of alumina and silica contained in the primitive. The skeletal densities were used to calculate the volume fractions of silica and alumina for each type of primitive, using the known densities of alumina powder and silica glass. This calculation is subject to some error arising from inaccurate skeletal density measurements due to closed porosity. The error tends to over estimate the amount of silica in each primitive and reduce the estimate of the alumina powder packing density within the primitive. The error is thought to be minor but the calculated alumina packing density reported here should be interpreted as a lower limit. Figure 5 shows the results of these calculations compared with the measured density of the powder bed for each powder. The alumina packing density in the primitives is substantially higher than the bed powder packing density in every case.

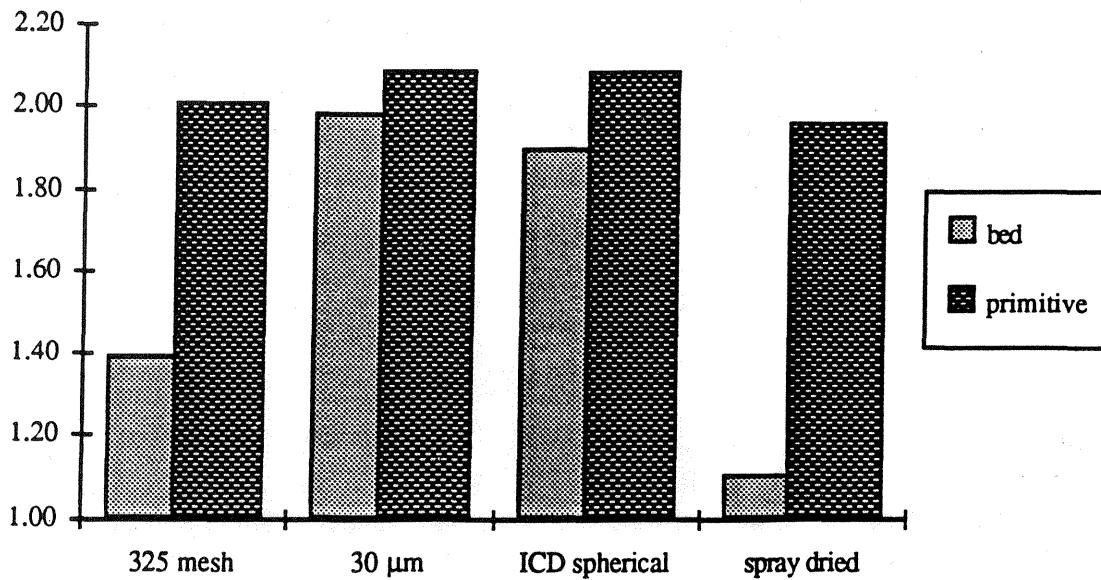


Table 5. Alumina packing (ml/g) in primitives vs. in the powder bed.

The generally spherical shape of the single droplet primitives is likely to be the result of liquid surface tension forces. Liquid coats the particles as the binder droplet penetrates the powder bed. Capillary pressure draws binder selectively into the necks between the particles. The liquid attempts to minimize its surface energy by reducing its surface to volume ratio and minimizing the area of liquid/vapor interface. The result is densification of the powder particles as the particles slide over one another in response to the surface tension of the liquid. Particles may be pulled together more tightly as the liquid dries causing further densification. The influence of surface tension forces will be greater in powder beds more susceptible to rearrangement, such as those with low initial packing densities or spherical particles which can rearrange much easier.

Figure 6 summarizes the measured bulk and skeletal densities for each kind of primitive. The bulk density increases in the order, spray-dried, solid spherical, 325 mesh, 30 micron. The skeletal density follows in exactly the reverse order, although it is much

less sensitive to powder type. Low skeletal density corresponds to high silica content, as discussed above. Thus, the alumina content of the primitives increases in order, spray-dried, solid spherical, 325 mesh, 30 micron.

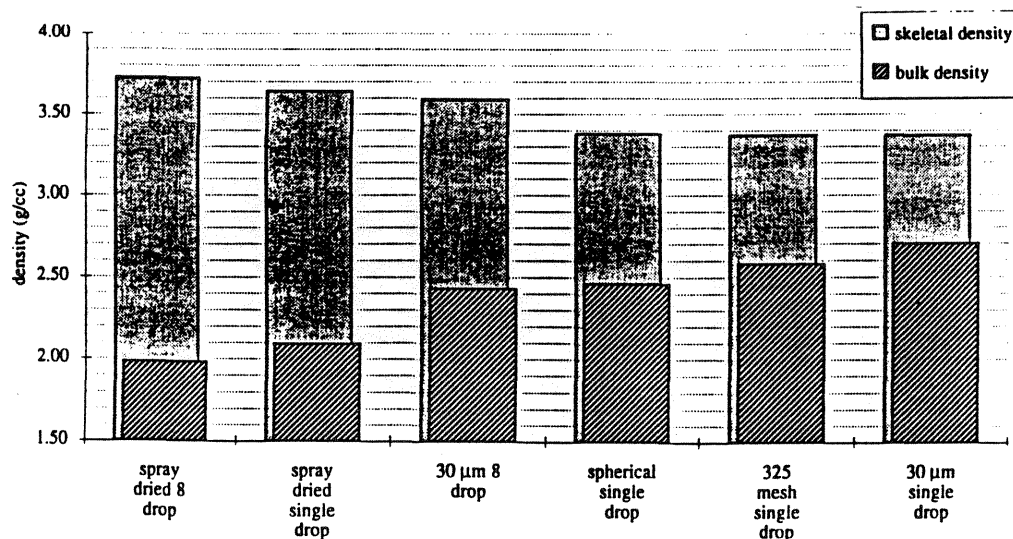


Figure 6. Summary of measured bulk and skeletal densities for primitive.

This observation is interesting given that each primitive is made from the same size binder droplet and must, therefore, contain the same total silica content. The data indicate that powder morphology controls the amount of alumina bound by a single binder droplet. A single binder droplet binds significantly more powder in the case of the spherical powders. The reason for this can be established by reference to Figures 3 and 4. Only small amounts of binder are required to bond the spherical particles since it readily segregates to the idealized two particle necks. Faceted particles, however, rearrange so that large flat surfaces face one another. Much more binder segregates to this type of neck because of its large surface area. Thus, for a given amount of binder, primitives from spherical powder should contain more alumina and should, therefore, be larger. Indeed, the primitives from the ICD spherical alumina were the largest of all the powders. The primitives from spray-dried alumina were not noticeably larger, but they undoubtedly were much less efficient in spreading binders because of their large amount of internal porosity.

The relationship between primitive structure and powder morphology is very important for the development of the 3D Printing process. We have established that spherical powders require much less binder than highly faceted powders. Thus, larger primitives are produced from spherical powders than from highly faceted particles for a given binder droplet size. This information has immediate impact on the development of materials for 3D Printing since it suggests that the minimum feature size that can be produced from spherical powders may be larger than that produced from highly faceted powders. This conclusion does not account for other effects such as the shrinkage which occurs due to capillary forces shown in Figure 5. The low packing density of the highly

faceted powders in the bed causes large amounts of linear shrinkage upon impact of the binder droplet. This effect will undoubtedly cause dimensional difficulties when fine structures are printed into faceted powders.

CONCLUSIONS

This study establishes the relationship between powder morphology and primitive structure. Significant increases in powder packing density can occur when binder droplets impact the powder bed. The particle rearrangement is caused by capillary forces created by liquid surface tension. The largest linear shrinkage will occur for powders with low packing density in the bed. Spherical powder efficiently uses binder since the necks between particles have small area and only small amounts of binder are required per neck to effectively bond the particles. High faceted powders have large area necks between particles which require much more binder per neck. The result of more efficient use of binder for the spherical powders is larger primitives for a given binder droplet size. Thus, each type of powder has advantages and disadvantages.

REFERENCES

1. Lauder A., M.J. Cima, E. Sachs, and T. Fan, "Three Dimensional Printing: Surface Finish and Microstructure of Rapid Prototyped Components"; in Proceedings, Synthesis and Processing of Ceramics: Scientific Issues, Boston, MA, 1991.
2. Fan T., A. Lauder, E. Sachs, and M.J. Cima, "The Surface Finish in Three Dimensional Printing," presented at the Third International Conference on Rapid Prototyping, University of Dayton, Dayton, OH 1992.
3. Cima M.J., and E. Sachs, "Three Dimensional Printing: Form, Materials, and Performance "; in Proceedings of the Solid Freeform Fabrication Symposium, Austin, TX, 1991.
4. Sachs E., M. Cima, J. Brecht, and Alain Cordeu, "CAD-Casting: The Direct Fabrication Ceramic Shells and Cores by Three Dimensional Printing," Manufacturing Review, vol. 5, no. 2, pp 117-126, June 1992
5. Sachs E., M. Cima, P. Williams, and D. Brancazio, "Rapid Tooling and Prototyping by Three Dimensional Printing," pp 41-45 in Transactions NAMRI/SME, 1990
6. Lauder A., "Microstructure and Particle Arrangement in Three Dimensional Printing," S.M. Thesis, Dept. of Materials Science and Engineering, Massachusetts Institute of Technology, September 1992